PHYSICAL REVIEW D VOLUME 27, NUMBER 3 1 FEBRUARY 1983

Zero-degree measurements of the inclusive reaction $np \rightarrow pX$ in the energy range 400 to 800 MeV

B. E. Bonner
Los Alamos National Laboratory, Los Alamos, New Mexico 87545

C. L. Hollas, C. R. Newsom,* and P. J. Riley
The University of Texas at Austin, Austin, Texas 78712

G. Glass, Mahavir Jain, and B. J. VerWest
Texas A&M University, College Station, Texas 77843
(Received 12 July 1982)

Differential cross sections $d^2\sigma/dp\,d\Omega$ have been measured near 0° for the inclusive reaction $np \rightarrow pX$, where X represents all possible combinations of pions and nucleons. Proton momentum spectra have been measured at average incident-neutron-momentum values from 950 to 1430 MeV/c in 60-MeV/c steps. Experimental results are compared with a field-theoretical peripheral model based on one-pion and ρ-meson exchange with nucleon-nucleon and nucleon-Δ intermediate states. The predictions of the model are in excellent agreement with the data, indicative that the $np \rightarrow pX$ reaction is dominated by the $p\Delta^0$ channel over the whole energy range of measurements.

I. INTRODUCTION

Single-pion production is the only significant inelastic channel in nucleon-nucleon collisions below 1 GeV. It is very important for understanding of the strong interaction in the medium-energy region, and many pion-production measurements have been performed,[1] particularly of the proton-proton reactions $pp \rightarrow pn\pi^+$ and $pp \rightarrow pp\pi^0$. The neutron-proton-induced reaction is much less studied, mostly because it is difficult to obtain monoenergetic neutron beams of sufficient intensity above pion threshold.

Recent $np \rightarrow \pi^+ X$ cross sections have been measured for neutron energies between 480 and 578 MeV at SIN by Kleinschmidt *et al.*[2] Inclusive $np \rightarrow pX$ angular-distribution measurements were reported by Bizard *et al.*[3] at Saclay, where the differential cross sections $d\sigma(np \rightarrow p\Delta_{33}^0)/dt$ have been determined from the experimental spectra at incident neutron momenta of 1.39, 1.56, 1.73, and 1.90 GeV/c. The inclusive reaction $np \rightarrow pX$ has also been studied by Glass *et al.*[4] at LAMPF at an incident energy of 800 MeV. Proton spectra were measured for angles between 0° and 31°. We report here measurements of the inclusive inelastic reaction $np \rightarrow pX$ near 0°, where X represents all possible combinations of pions and nucleons. Proton momentum spectra have been measured at average incident-neutron-momentum values from 950 to 1430 MeV/c. The measurements, carried out in 60-MeV/c steps, complement the earlier $np \rightarrow pX$ data at 800 MeV reported by Glass *et al.*[4] and enhance the coverage of the Saclay data.

Bizard *et al.*[3] have calculated the momentum distribution for the inclusive reaction $np \rightarrow pX^0$ using the one-pion-exchange (OPE) formalism of Ferrari and Selleri[5] applied to the reaction $NN \rightarrow NN\pi$ and modified by the parametrization of Benecke, Durr, and Pilkuhn.[6,7] They conclude that the model gives a reasonable interpretation of the measured $d^2\sigma(np \rightarrow pX)/d\Omega\,dp$ momentum spectra, both for the shape and the absolute normalization. However, the variation of the $d\sigma(np \rightarrow p\Delta_{33}^0)/dt$ cross sections as a function of t, determined by subtraction of nonresonant background from these spectra, differs from the OPE predictions particularly for small values of t. The deduced $d\sigma(np \rightarrow p\Delta_{33}^0)/dt$ differential cross sections show a dip for small values of t, rather than the peak predicted by the OPE calculation. This dip implies the existence of a mechanism other than one-pion exchange in Δ_{33} production, as has been shown to be the case in the charge-exchange $np \rightarrow pn$ reaction.[8]

II. EXPERIMENTAL METHOD

The present measurements were carried out as part of an experiment[9] designed to study the s and u variations of the np charge-exchange cross sections over the range $575 < P_n < 1429$ MeV/c. The experiment uses a continuum beam of neutrons from the reaction $p + \mathrm{Al} \rightarrow n + X$ incident on a liquid-

hydrogen target. Recoiling protons are detected with a multiwire proportional chamber spectrometer. The spectrometer has been described previously.[10,11] Briefly, the 800-MeV proton beam at the Clinton P. Anderson Meson Physics Facility (LAMPF) passes through a 2-cm-thick aluminum target and after deflection through 60° is transported to a beam dump several meters away. Neutrons emerging at 0° are collimated to form a neutron beam, which is then cleared of charged particles by a sweep magnet. The spectrum of neutrons thus obtained is characterized by a peak above 1400 MeV/c and a broad continuum of neutrons at lower momenta.[11] Charged particles emerging from the interaction of the neutron beam with a liquid-hydrogen target are momentum analyzed in the spectrometer. Particle identification is accomplished by a simultaneous measurement of their time of flight through the spectrometer, which allows a calculation of the particle mass by the usual relation $M=P/\beta\gamma$. Particle identification is unambiguous for greater than 99% of the events. The angular acceptance in the present work is approximately 4° (−2° to +2°).

Once the protons are identified, the proton momentum and angle for the elastic events uniquely specify the incident neutron momentum associated with each event. For an inelastic event, such as $np\rightarrow np\pi^-$, there is no such one-to-one correspondence. However, the incident neutron time of flight is measured in addition to the proton momentum. This time-of-flight measurement not only allows the elastic and inelastic events to be easily separated, but also provides a determination of the incident neutron momentum associated with inelastic proton events. The time resolution ($\simeq$1 nsec) and flight path ($\simeq$10 m) resulted in an uncertainty in the incident neutron momentum of approximately 2%. After the neutron momentum is calculated from the measured time of flight, the inelastic protons are sorted into nine bins, each 60 MeV/c wide, corresponding to events whose average incident neutron momentum lies between 950 and 1430 MeV/c (at energies of 396, 440, 484, 530, 577, 624, 673, 722, and 772 MeV). An inelastic proton momentum spectrum is obtained for each neutron momentum interval; these are shown in Fig. 1.

Absolute cross sections are determined from the yield of deuterons detected simultaneously from the reaction $np\rightarrow d\pi^0$, as described in Ref. 9. Since the cross section for $np\rightarrow d\pi^0$ is assumed from charge independence to be one-half that for the well-known[12] reaction $pp\rightarrow d\pi^+$, it is possible to calculate from the detected deuterons the product of the number of incident neutrons in each bin and the number of target atoms per unit area. Given this product, the absolute differential cross section can be obtained.

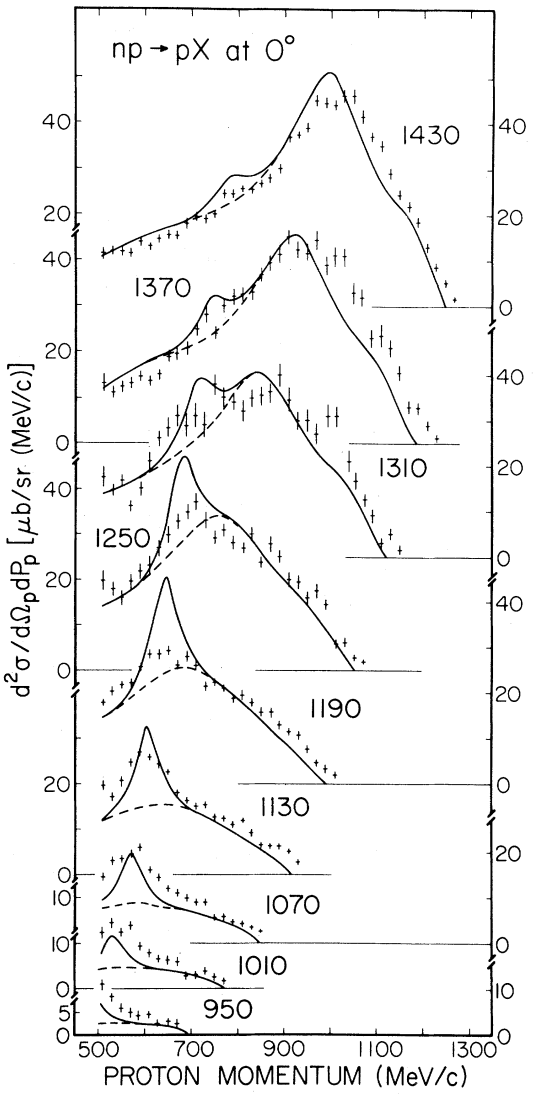

FIG. 1. Proton momentum spectra at $\theta_L=0°$ measured in this experiment. The average incident neutron momentum is indicated for each spectrum in MeV/c. These momentum values correspond to energies of 396, 440, 484, 530, 577, 624, 673, 722, and 772 MeV, respectively. The curves give the peripheral-model predictions with (solid curve) and without (dashed curve) nucleon-nucleon final-state interactions.

Corrections to the data included those for dead-time effects in the data-acquisition system (<10%) and deuteron loss resulting from collisions in the scattering target and spectrometer (2.5 to 3.5%). Spectrometer inefficiencies were measured to be substantially less than 1% and were neglected. We estimate the overall systematic errors, including normalization error, to be approximately 10%.

III. DISCUSSION

In order to identify the dominant features of the data, these results are compared with a field-theoretical peripheral model based on one-pion and ρ-meson exchange with nucleon-nucleon and nucleon-Δ intermediate states.[13,14] The nucleon-nucleon final-state interaction in this calculation has been handled in a qualitative way following the approach of Goldberger and Watson.[15] The helicity amplitudes are transformed into the final-state NN c.m. frame, and the amplitudes for NN spin 0 and 1 are then constructed. The Goldberger-Watson final-state-enhancement factor can be written as

$$f(k)=\frac{(k^2+\alpha^2)}{1/a+\frac{1}{2}rk^2-ik}\left[\frac{r}{2}\right],$$

where a and r are the scattering length and effective range and

$$\alpha=\frac{1}{r}+\left[\frac{1}{r^2}-\frac{2}{ar}\right]^{1/2}.$$

We are interested only in the qualitative effects of the scattering length region and thus have restricted the effect of the enhancement factor to final states with $k<k_0$ where k_0 is a cutoff momentum. Since for very low energies the spin-1 and spin-0 amplitudes are predominantly $^1S_0$ and $^3S_1$, respectively, we can apply these factors directly to the amplitudes $M_0(k)$,

$$M(k)=[f(k)/f(k_0)]M_0(k), \quad k<k_0$$
$$=M_0(k), \quad k\geq k_0,$$

where $M(k)$ is the relevant modified amplitude. Standard values for the effective ranges and scattering lengths are used; $k_0=0.45$ fm^{-1} is taken from Ref. 13 where it is adjusted to fit the data at 800 MeV.

The most striking features in the proton momentum spectra in Fig. 1 are the peaks that move from below 500 MeV/c at the lowest energy to near 1000 MeV/c at the highest incident neutron energy. These peaks show the energy dependence of the low-energy nucleon-nucleon and π-nucleon interactions in the final state. The first peak to appear with increasing energy is attributable to low-energy nucleon-nucleon phenomenology. Below an incident momentum of $P_L=1250$ MeV/c (624 MeV) this is the only distinguishable feature. Above $P_L=1250$ MeV/c a second peak appears at a slightly higher proton momentum and rapidly dominates the spectrum. At $P_L=1430$ MeV/c, the low-energy nucleon-nucleon peak has diminished to a shoulder on this higher peak. This prominent peak, which occurs for πN energies slightly below 1232 MeV, is a manifestation of the 1232-MeV Δ resonance that dominates this reaction. The main process seen here is the charge-exchange reaction $np\rightarrow p\Delta^0$, shown schematically in Fig. 2.

Figure 3 shows the virtual-pion four-momentum squared as a function of T_L for various πN invariant energies. Of particular interest is the curve for a πN energy of 1200 MeV, which is close to the value at the peak. The curve starts at about 560 MeV, and indicates that below this energy the πN subsystem cannot be formed with 1200-MeV invariant energy. Between 560 and 650 MeV the momentum transfer (the invariant mass of the virtual, or exchanged pion) decreases in magnitude very rapidly as the

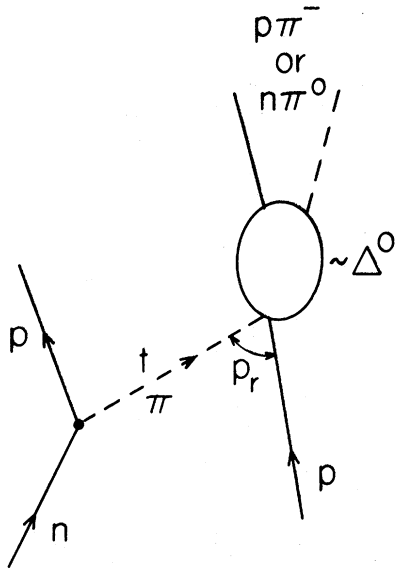

FIG. 2. The dominant process for the reaction $np\rightarrow pX$ in this energy range.

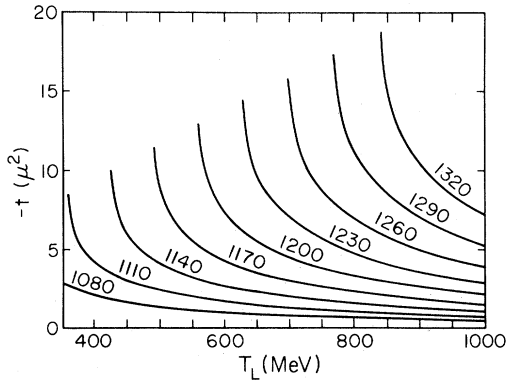

FIG. 3. The invariant mass ($t=-q_\pi{}^2$) of the off-shell pion in the πN amplitude shown in Fig. 2 plotted as a function of incident neutron energy T_L. The curves are for $np\rightarrow p(\pi N)$ at $\theta_L=0°$ and for various πN center-of-mass energies that are indicated in MeV on each curve.

pion propagator approaches the on-shell value of $-t=\mu^2$ from far off shell. Therefore, as T_L increases from 560 to 650 MeV, the resonance peak from the Δ appears and quickly dominates the spectra. Above 650 MeV, $-t$ approaches 0 gradually and the peak structure changes more slowly. The disappearance of the Δ peak below 650 MeV does not imply that the $np\to p\Delta^0$ mechanism is no longer important. Because of its large width (full width at half maximum$\simeq$115 MeV), the $p\Delta^0$ channel can still couple to the $np\to pX$ reaction with small momentum transfer down to about 400 MeV, as indicated in Fig. 3. Thus at low energies the reaction continues to be dominated by the off-resonance Δ channel, with a peak coming from final-state nucleon-nucleon interaction.

In order to demonstrate the Δ dominance, even below resonance, the peripheral model results without nucleon-nucleon final-state interactions are also plotted in Fig. 1. The nucleon-nucleon final-state interaction is handled only approximately, and is clearly too large near 1190 MeV/c, but it indicates the location and general energy dependence of that peak. The energy dependence of the underlying production mechanism (one-pion exchange in $np\to p\Delta^0$) reproduces the general features of the spectra very well except for the very lowest energies.

In the present work we varied the momentum transfer (the invariant pion mass) by changing the incident energy at a fixed scattering angle; Fig. 3 shows the momentum-transfer region reached in the experiment. In most experiments, the momentum transfer has been varied by changing the scattering angle of the forward scattered proton. Thus the present measurements and the inclusive data[4] at $T_L=794$ MeV provide two complementary experiments investigating the off-shell form of the πN amplitude.

The integrated 0° cross sections

$$\int_{p_0}^{p_{\max}} dp \frac{d^2\sigma}{dp\, d\Omega}$$

are shown in Fig. 4 together with the corresponding 0° and 1.5° integrated cross sections from the $np\to pX$ measurements of Refs. 3 and 4. For comparison purposes we also show the 0° $pp\to nX$ data of Ref. 1. The agreement between the present data, the work of Bizard *et al.*,[3] and that of Glass *et al.*[4] is excellent; the data indicate a smooth rise in the 0° cross sections from just above the pion-production threshold at 0.78 GeV/c to the highest energy of the Bizard measurement at 1.9 GeV/c. Predictions from the peripheral-model calculation for both $np\to pX$ and $pp\to nX$ agree well with the data shown except between threshold and 1.13 GeV/c, where the model is slightly below the data.

The πNN vertex has been extensively studied with other reactions and has a momentum-transfer dependence of the form[16]

$$\Gamma(q^2)=\frac{\Lambda^2-\mu^2}{\Lambda^2-q^2}\ ,$$

where $\Lambda\simeq 900$ MeV. The πN amplitudes used in common separable potential models or in Chew-Low theory[17] decrease in magnitude very rapidly as one goes off shell in the one-pion leg ($q^2=-t\neq\mu^2$). When such models are used in the peripheral calculations the spectra predicted are in good agreement with experiments near 0° at 800 MeV, but they become too small as one increases the momentum transfer by decreasing the energy or by increasing the scattering angle. This has the effect of producing a steeper slope in Fig. 4, contrary to experimental results. This discrepancy suggests a different dependence of the amplitude on the off-shell pion momentum than that which comes from the above models. The implied $q^2(-t)$ dependence seen in the present experiments is relatively flat beyond about $-t\simeq 8\mu^2$. The current models for the πN amplitudes work well for momentum transfers of magnitude less than $8\mu^2$, but for $-t>8\mu^2$ new processes

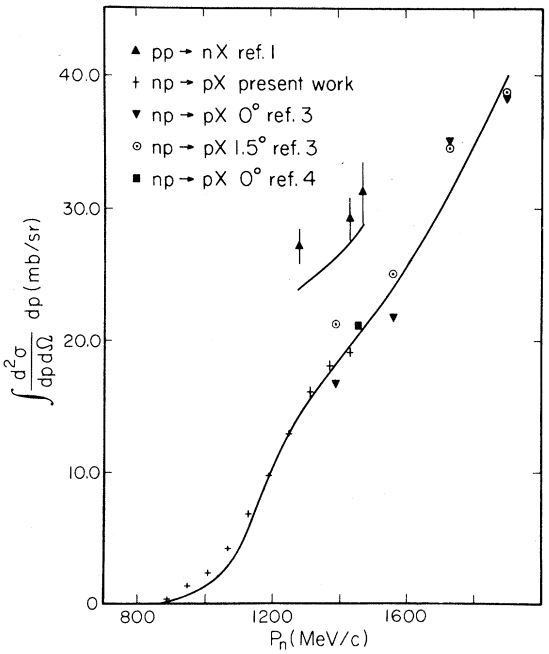

FIG. 4. Integrated $\theta_L=0°$ cross section

$$\int_{p_0}^{p_{\max}} dp \frac{d^2\sigma}{dp\, d\Omega}\ ,$$

where $p_0=500$ MeV/c and $p_{\max}$ is the upper phase-space limit. The curves are from the peripheral-model predictions as in Fig. 1. The same value of p_0 is used for all the data shown in the figure.

must dominate the πN amplitudes, which have a very weak $-t$ dependence. This weak $-t$ dependence appears in the peripheral model used in the present analysis as large cutoff masses in form factors and an adjusted $\pi N\Delta$ coupling constant. This model leads to the wrong πN on-shell amplitude, using a Chew-Low-type extrapolation. However, the production reaction is not sensitive to the on-shell value, and is instead a direct measure of the off-shell amplitude. Additional work is required to refine the further extraction of information about the on-shell πN amplitude from this reaction, but the present data set promises to be a valuable and unique source of new information about the off-shell πN amplitude. Knowledge of off-shell behavior is also important, since this process is the dominant one for producing pions in nucleon-nucleus collisions. Work following these lines may lead to an improved model for the production operator in reactions with nuclei.

ACKNOWLEDGMENTS

Support of the LAMPF staff at all stages of setup and performance was greatly appreciated.

We give special thanks to Paul Allison and Ralph Stevens for the design and development of the LAMPF chopped-beam system. We express our gratitude to J. E. Simmons, L. C. Northcliffe, J. C. Hiebert, and others who participated in the development of the spectrometer system of the LAMPF Nucleon Physics Laboratory. This work was supported by the U. S. Department of Energy.

---

*Present address: Laboratorie National Saturne, 91190 Gif-sur-Yvette, Cedex, France.

[1]G. Glass *et al.*, Phys. Rev. D 15, 36 (1977), and Refs. 10—24 therein.

[2]M. Kleinschmidt *et al.*, Z. Phys. A 298, 253 (1980).

[3]G. Bizard *et al.*, Nucl. Phys. B108, 189 (1976).

[4]G. Glass, *et al.*, in *Nucleon-Nucleon Interactions—1977,* Proceedings of the Second International Conference, Vancouver, edited by H. Fearing, D. Measday, and A. Strathdee (AIP, New York, 1978), p. 544; and (unpublished).

[5]E. Ferrari and F. Selleri, Nuovo Cimento 27, 1450 (1963).

[6]H. P. Durr and H. Pilkuhn, Nuovo Cimento 40, 899 (1965).

[7]J. Benecke and H. P. Durr, Nuovo Cimento 56, 269 (1968).

[8]R. J. N. Phillips, Phys. Lett. 4, 19, (1963).

[9]B. E. Bonner *et al.*, Phys. Rev. Lett. 41, 1200 (1978).

[10]M. L. Evans *et al.*, Phys. Rev. Lett. 36, 497 (1976).

[11]B. E. Bonner *et al.*, Phys. Rev. C 18, 1418 (1978).

[12]C. Richard-Serre *et al.*, Nucl. Phys. B20, 413 (1970).

[13]B. J. VerWest, Phys. Lett. 83B, 161 (1979).

[14]J. H. Gruben and B. J. VerWest, TAMU Report No. DOE/ER/05223-44, 1981 (unpublished).

[15]M. L. Goldberger and K. M. Watson, *Collision Theory* (Wiley, New York, 1969), p. 549.

[16]C. A. Dominguez and B. J. VerWest, Phys. Lett. 89B, 333 (1980).

[17]G. F. Chew and F. W. Low, Phys. Rev. 101, 1570 (1956).